Modified H∞ loop-shaping procedure for the two degrees-of-freedom control configuration of an UAV (ARCHER V 1.7)

Adrian BURGHIU*,[1], Adrian-Mihail STOICA[2]

*Corresponding author
[1]INCAS – National Institute for Aerospace Research "Elie Carafoli",
Iuliu Maniu Blvd. 220, 061126 Bucharest, Romania,
burghiu.adrian@incas.ro*, burghiu_adrian@yahoo.com
[2]Faculty of Aerospace Engineering,
National University of Science and Technology POLITEHNICA Bucharest,
Gheorghe Polizu 1-7, 011061 Bucharest, Romania,
stoica.am@gmail.com

DOI: 10.13111/2066-8201.2025.17.4.2

Received: 27 October 2025/ Accepted: 12 November 2025/ Published: December 2025

Abstract: *The robust stabilization problem with respect to both dynamic and parametric uncertainty for linear deterministic systems is analyzed in the present article. The robust design methods consider either the dynamic modelling in frequency domain of the uncertainty or, its parametric representation in the state space realisation. Suitable analysis approaches for parametric uncertainty modelling are provided by Kharitonov and Edge-type theorems. Under some specific assumptions, these methods allow to determine the whole admissible domain of the uncertain parameters for which a system is stable. It shall describe a method that combines the advantages of the control techniques with ones given by the polytopic representation of parametric uncertainty. A modified H_∞ loop-shaping approach allowing to solve control problems in which robust stabilization, sensitivity reduction, and model following design objectives are formulated is presented and it allows to handle tracking design specifications. The modified loop-shaping procedure allows to design a controller that provides a) robust stability with respect to the normalized left coprime factorization (NLCF); b) reduced sensitivity with respect to output disturbance on a specified range of frequencies, and c) tracking of the output of a given ideal model. The article is finished with a case study in which a two degrees-of-freedom control system with respect to the pitch angle for the longitudinal dynamics of a UAV (ARCHER V1.7) is designed using the modified H_∞ loop-shaping procedure.*

Key Words*: modified H∞ loop-shaping, robust stability, robust design methods, robust stabilization, linear deterministic systems.*

1. INTRODUCTION

Robust flight control for Unmanned Aerial Vehicles (UAVs) remains a major research topic due to the strong dependence of aerodynamic characteristics on flight speed, altitude, and manoeuvring conditions [1], [2], [3]. These variations often reduce short - period damping or may even lead to open-loop instability in the pitch axis. At the same time, modern UAV missions, including autonomous takeoff and landing, terrain-following, and loiter

stabilization, require precise pitch attitude regulation provided by autopilot modes such as Stability Augmentation System (SAS) and Pitch Attitude Hold (PAH) [4], [5].

H_∞ loop-shaping provides a powerful approach to achieving robust stabilization in the presence of modeling uncertainty, using normalized coprime-factor tools for guaranteed stability margins [6], [7]. However, classical loop-shaping does not explicitly enforce trajectory-tracking constraints. A modified H_∞ loop-shaping procedure has therefore been developed in the literature to incorporate model-following requirements through a two-degrees-of-freedom (2-DoF) controller structure [8], [9], [10]. This configuration allows simultaneous satisfaction of three key design objectives: robust stability with respect to dynamic uncertainty, disturbance-rejection through sensitivity shaping, and accurate following of an ideal reference model.

Operating-point variations remain a critical aspect in UAV control design. A common remedy is to formulate the controller in a Linear Parameter-Varying (LPV) representation, using polytopic interpolation to guarantee smooth scheduling as the flight condition evolves [11], [12], [13], [14]. In this paper, we adopt this approach for the ARCHER V1.7 fixed-wing UAV longitudinal axis. Four flight conditions at sea level are considered, and an H_∞-based 2-DoF controller is synthesized for each. Numerical simulations demonstrate excellent pitch tracking and stability characteristics across the full operating range.

2. BACKGROUND AND MODIFIED H∞ LOOP-SHAPING METHODOLOGY

Classical H_∞ loop-shaping proceeds in two steps. First, the nominal loop is shaped with suitable weights to achieve desirable bandwidth and high-frequency roll-off. Second, an H_∞ synthesis guarantees robust stability with respect to normalized coprime-factor (NCF) uncertainty [6], [7], [15]. The obtained H_∞ bound γ provides a certified robustness margin because closed-loop stability is preserved for all normalized multiplicative uncertainties Δ satisfying $\|\Delta\|_\infty < 1/\gamma$. This explicit stability guarantee is a practical advantage when dealing with modeling errors or operating-point variability.

The classical design does not directly address trajectory tracking. To incorporate performance constraints on the pitch attitude response, a two-degrees-of-freedom controller structure is used [8], [9], [10], [16]. The total controller is expressed as:

$$K(s) = [K_1(s)\ K_2(s)] \tag{1}$$

where $K_1(s)$ shapes the nominal feedback loop and ensures robustness, while $K_2(s)$ introduces explicit model-following ability.

The sensitivity and the complementary sensitivity functions are defined as:

$$S(s) = (I + G(s)K_1(s))^{-1} \tag{2}$$

$$T(s) = I - S(s). \tag{3}$$

The objective of $K_1(s)$ is to minimize $S(s)$ at low and mid frequencies while ensuring that $T(s)$ decays at high frequency, preventing noise amplification and poor actuator usage.

Tracking is driven by the filtered model-following error:

$$e(t) = \theta(t) - \theta_{model}(t) \tag{4}$$

$$z(t) = W_e(s)e(t) \tag{5}$$

where $\theta_{model}(t)$ stands for the output of a model chosen according to the specifications for the time response performance of the pith angle $\theta(t)$ of the UAV. The filter $W_e(s)$ is used to encode desired transient response, such as limited overshoot and short settling time, and to enforce bandwidth shaping. Minimizing the transfer from disturbances to $z(t)$ in the H_∞ sense ensures that the pitch attitude $\theta(t)$ closely follows the reference model, while still satisfying robustness requirements.

The structure of the modified H_∞ loop-shaping 2-DoF controller is illustrated in Fig. 1.

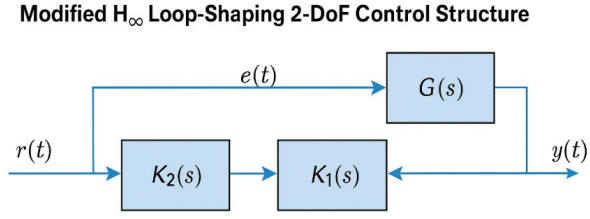

Fig. 1: Control structure scheme

An ideal reference model $H_{model}(s)$, chosen with pilot-like damping and rise time, defines the desired PAH-quality behavior. $K_2(s)$ enforces tracking while $K_1(s)$ maintains robust stability. Since aerodynamic derivatives vary significantly with airspeed, the four fixed-speed controllers are embedded into a polytopic LPV scheduling structure [11], [12], [13], [14]. This guarantees smooth variation of performance as the UAV accelerates or decelerates, without switching behaviour or degradation of stability margins.

3. UAV LONGITUDINAL MODEL

The ARCHER V1.7 is a small fixed-wing UAV designed for autonomous surveillance missions under low-speed conditions. The longitudinal dynamics can be accurately captured using a four-state representation describing variations from trimmed flight. The state vector is defined as:

$$x(t) = \begin{bmatrix} u(t) \\ \alpha(t) \\ q(t) \\ \theta(t) \end{bmatrix}, \tag{6}$$

where u denotes the forward speed deviation from its value corresponding to the trimming conditions, α is angle of attack, q is pitch rate, and θ is pitch angle. The elevator deflection δ_e is the control input generating pitch control moments.

The model is obtained by linearizing the nonlinear 6-DoF equations of motion around trimmed straight-and-level flight conditions using stability and control derivatives evaluated from the ARCHER aerodynamic database supported by a combination of CFD analysis and wind-tunnel validation.

The linear time-invariant (LTI) model used at each operating point is given by:

$$\dot{x}(t) = A(V)x(t) + B(V)\delta_e(t) \tag{7}$$

$$\theta(t) = Cx(t) \tag{8}$$

where the airspeed V acts as a scheduling parameter, reflecting aerodynamic variations.

Four trimmed speeds spanning the relevant operating range at sea level are considered:

Table 1: Trimmed flight conditions at sea level

Case	Airspeed (V) [m/s]	Angle of attack (α) [deg]	Pitch angle (θ) [deg]	Elevator deflection (δ_e) [deg]
1	26.0	7.2	7.1	2.5
2	31.5	5.8	5.7	1.6
3	35.0	4.9	4.8	1.1
4	39.0	4.0	3.9	0.8

The longitudinal dynamics feature two well-known modes: the short-period mode, dominated by angle-of-attack and pitch-rate coupling and directly responsible for pitch stability, and the phugoid mode, representing slow oscillations driven by speed–altitude energy exchange. For the present UAV configuration, the short-period mode exhibits reduced damping at higher airspeeds, which can negatively affect open-loop flight qualities.

Fig. 2 illustrates the variation of the short-period damping ratio extracted from the dominant complex closed-loop poles at each design point. A decreasing trend is observed as airspeed increases, confirming the need for stability augmentation through an automatic control system.

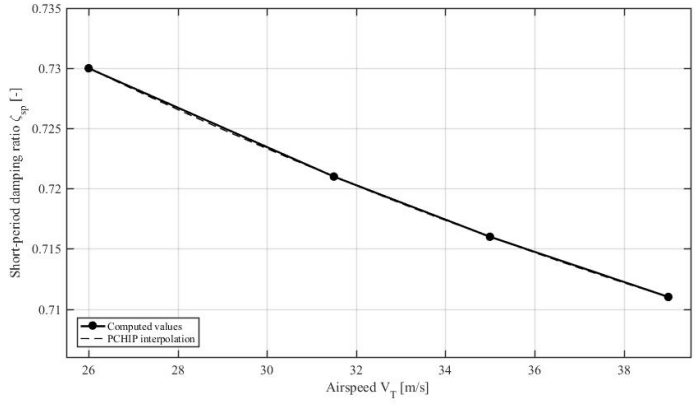

Fig. 2: Short-period damping ratio vs airspeed. Damping computed from the dominant complex pole pair at each design speed (26, 31.5, 35, 39 m/s).

The short-period damping decreases mildly with airspeed, which motivates the need for robust stabilization across the envelope.

The linearized models remain suitable for small perturbations around the trim conditions, consistent with typical SAS (Stability Augmentation System) and PAH (Pitch Attitude Hold) autopilot objectives. To extend the validity of the control design throughout the operational range, four individually tuned controllers will be combined in Section 5 using a polytopic LPV scheduling approach.

4. CONTROLLER DESIGN AND NUMERICAL RESULTS

The modified H_∞ loop-shaping synthesis was carried out for each of the four trimmed models previously defined. The design relies on loop-shaping filters that modify the open-loop frequency response so that the shaped plant satisfies performance targets before robust stabilization is applied. A pre-compensator $W_1(s)$ is used to increase low-frequency gain and

enhance disturbance rejection and model-following accuracy, while a post-compensator $W_2(s)$ is optionally employed to shape the high-frequency roll-off and reduce sensitivity to sensor noise. Let the shaped plant be defined as:

$$G_s(s) = W_2(s)G(s)W_1(s) \tag{9}$$

and let $K_s(s)$ denote the stabilizing H_∞ controller for $G_s(s)$ The resulting 2-DoF loop-shaping controller is given by:

$$K_1(s) = W_1(s)K_s(s) \tag{10}$$

$$K_2(s) = C(s)K_s(s) \tag{11}$$

where $C(s)$ represents the model-following compensator, acting on the filtered tracking error signal described previously.

Robust stability with respect to normalized coprime-factor (NCF) uncertainty is certified by ensuring:

$$\|T_{zw}(s)\|_\infty < \gamma \tag{12}$$

which guarantees that the closed-loop system maintains internal stability for any admissible perturbation $\Delta(s)$ satisfying $\|\Delta\|_\infty 1/\gamma$. This explicit measure of robustness is a powerful actuator in flight control design because it provides analytical margins against unmodeled aerodynamics, sensor bias, environmental disturbances, and parameter variations [6], [7].

The outer-loop controller $K_2(s)$ enforces the ideal reference dynamics by minimizing the transfer function from disturbance-to-output and reference-to-error. As a result, the closed-loop response achieves reduced overshoot and rapid convergence to the commanded pitch attitude.

At each airspeed, the synthesis yields a distinct pair of controllers:

$$\{[K_1(V_i), K_2(V_i)]\}, \quad i = 1,2,3,4 \tag{13}$$

associated with the four trimmed operating conditions.

Because the aerodynamic derivatives change monotonically with airspeed, the family of controllers is embedded in a polytopic LPV (Linear Parameter-Varying) representation. The airspeed V is used as a scheduling parameter and the global controller is obtained through a third-degree polynomial interpolation in airspeed:

$$K(V) = a_0 + a_1V + a_2V^2 + a_3V^3 \tag{14}$$

where the coefficients a_i are identified such that $K(V_i) = K_i$ for each design speed $V_i \in \{26, 31.5, 35, 39\}\, m/s$. This polynomial fitting ensures smooth gain scheduling with continuous first and second derivatives, avoiding abrupt slope changes that may arise with piecewise linear blending.

This approach guarantees smooth and continuous control action throughout the flight envelope. The closed-loop stability is preserved for all $V \in [26,39]\, m/s$ within the interpolation range, without the need for gain switching, thus preventing undesired transients that could compromise flight safety.

The LPV scheduling also reduces controller redesign effort, since only the four vertex controllers are synthesized explicitly [11], [12], [13], [14].

In conclusion, the loop-shaping process preserves internal stability and disturbance rejection while the model-following stage ensures that tracking performance remains uniform across airspeed variations.

This combined structure is particularly suited for Pitch Attitude Hold (PAH) autopilots installed on lightweight UAVs.

The frequency-domain requirements, including low sensitivity $S(s)$ in the low-to-mid range and fast roll-off of $T(s)$ in the high-frequency region, are fulfilled by the H_∞ loop-shaping step previously detailed.

These properties are confirmed indirectly by the achieved time-domain performance, where disturbance rejection and actuator protection are ensured without excessive control activity or noise amplification. The resulting feedback loop satisfies the robustness margin guaranteed by the normalized coprime-factor framework.

Numerical simulations were performed at the four design speeds and, additionally, at intermediate flight conditions using the scheduled controller $K(V)$. For each operating point a 1 radian pitch attitude step was applied, and performance was assessed in terms of the tracking error $e(t) = \theta(t) - \theta_{model}(t)$, the maximum transient deviation, and the 2% settling time. The four nominal results are reported in Fig. 3–6, which consistently show milliradian-level errors and virtually zero settling time. A mild degradation with increasing speed is observed, which is consistent with the short-period damping evolution in Fig. 2 and reflects the expected shift in aircraft dynamics.

The LPV scheduling was then exercised between the design points to confirm that the controller maintains uniform behaviour under smooth variations of the airspeed. In practice, this is the operating regime of the autopilot, as the vehicle accelerates or decelerates during typical mission segments (e.g., climbs, descents, or level-flight speed changes). To provide a concise view of the scheduled performance, Fig. 7 summarizes the maximum tracking error versus airspeed, including intermediate speeds obtained by interpolation. The monotonic trend and the tight error bounds confirm that the interpolated controller retains the desired performance between vertices. No switching transients were observed and the performance curves are smooth, which is precisely the intended behaviour of an LPV gain-scheduled design.

From a robustness standpoint, the time-domain results are consistent with the frequency-domain shaping enforced by the modified H_∞ approach: low sensitivity in the low-to-mid frequency range translates into rapid disturbance rejection, while the high-frequency roll-off of the complementary sensitivity limits actuator activity and noise amplification. The overall effect is a pilot-like pitch attitude response across the full speed range, suitable for PAH autopilot operation on the ARCHER V1.7 UAV.

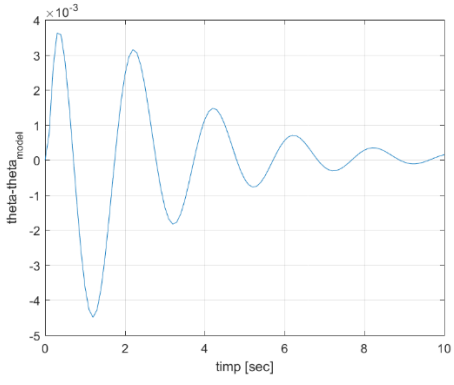

Fig. 3: Tracking error for V = 26.0 m/s.

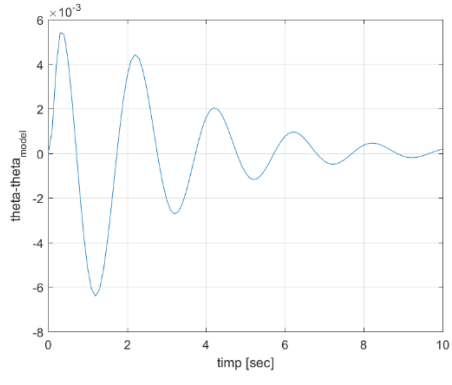

Fig. 4: Tracking error for V = 31.5 m/s.

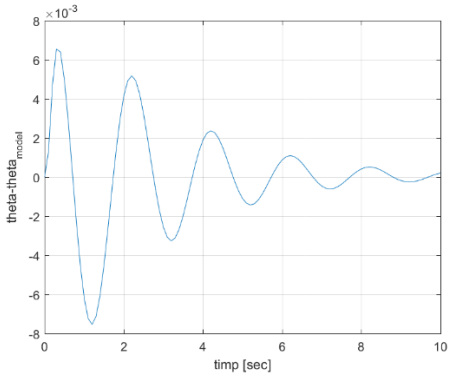

Fig. 5: Tracking error for V = 35.0 m/s.

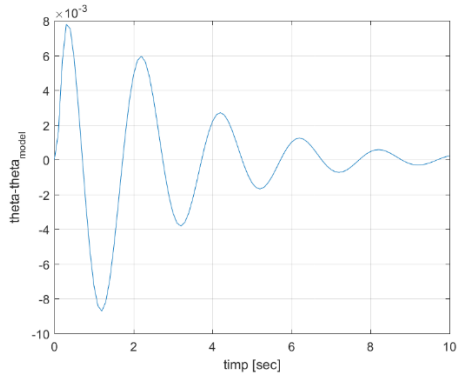

Fig. 6: Tracking error for V = 39.0 m/s.

Table 2 summarizes the the maximum tracking error versus airspeed.

Table 2: Nominal performance at the design points

Airspeed V [m/s]	Max. error [rad]
26.0	4.49×10^{-3}
31.5	6.41×10^{-3}
35.0	7.54×10^{-3}
39.0	8.71×10^{-3}

To visualize the speed-wise performance continuity, Figure 7 reports the maximum tracking error as a function of airspeed, combining the four nominal points with interpolated values obtained between them. The resulting profile is smooth and bounded, which supports the claim that the LPV interpolation preserves the closed-loop behaviour across the entire operating interval.

The curve is nearly linear and remains in the milliradian range, which confirms that the scheduled design preserves tight model-following while the airspeed changes continuously between operating points.

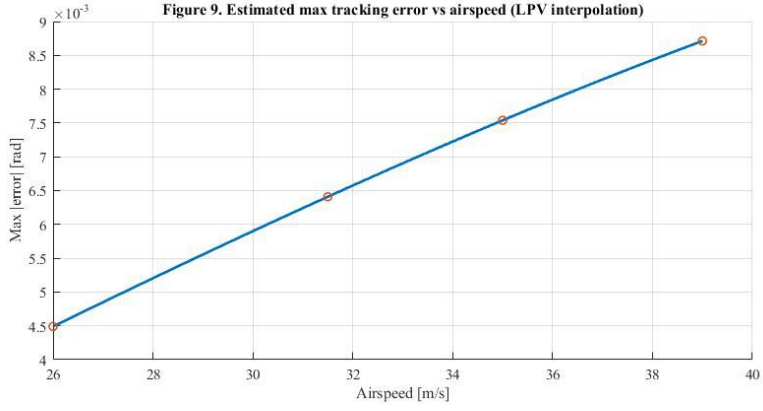

Fig. 7: Estimated max tracking error vs airspeed (LPV interpolation). - Values obtained by interpolating the scheduled controller between the four design speeds; the monotonic trend confirms smooth performance variation across the envelope.

The curve includes the four nominal results and interpolated values at intermediate speeds; the trend remains smooth and within the desired bounds.

Finally, Fig. 8 shows the closed-loop poles at the four design speeds. All poles lie in the left half-plane, with damping consistent with Fig. 2, which confirms internal stability throughout the envelope.

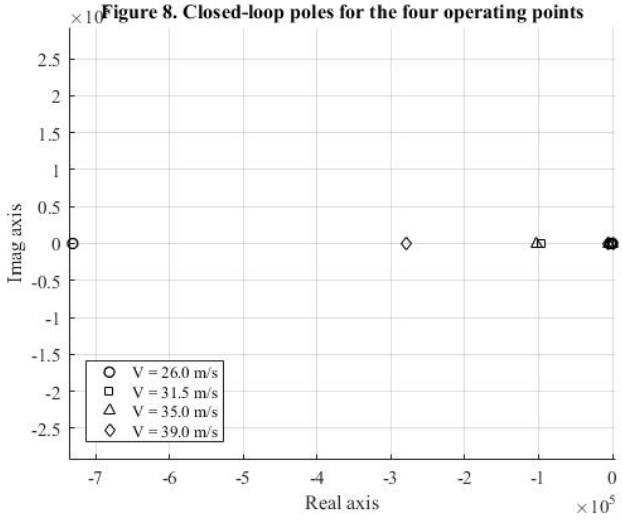

Fig. 8: Closed-loop poles at the four controlled operating points.

Fig. 8 shows that all closed-loop poles are located very far in the left half-plane, with real parts on the order of 10^5. This indicates a highly damped closed-loop system with negligible oscillatory content. Differences across the four airspeeds are minimal, confirming strong gain and phase margins and consistent stability performance throughout the flight envelope.

These results confirm that the modified H_∞ loop-shaping, combined with polytopic LPV scheduling, delivers robust stability, smooth performance variation, and precise model-following for the UAV pitch attitude control problem.

5. CONCLUSIONS

This paper proposed a modified H∞ loop-shaping 2-DoF control design for pitch-attitude stabilization of the ARCHER V1.7 UAV. A family of controllers was synthesized at four representative airspeeds and embedded within a polytopic LPV scheduling framework based on the measured flight speed. The resulting scheduled controller preserves the robust stability guarantees of the normalized coprime-factor approach while maintaining uniform closed-loop behaviour throughout the envelope.

The numerical simulations demonstrated excellent tracking accuracy, with peak errors below 10 milliradians and nearly zero settling time across all tested airspeeds. Closed-loop pole analysis confirmed a highly damped and stable dynamic response, and intermediate-speed simulations validated the smooth interpolation property required for reliable LPV scheduling. These results show that the proposed approach fully satisfies pitch-attitude autopilot requirements, ensuring precise command following without inducing excessive control effort.

The improved attitude stability contributes directly to maintaining the aircraft at efficient angles-of-attack, helping reduce unnecessary control deflections and thereby supporting enhanced mission endurance for surveillance operations. Future work will focus on extending the controller to the full 6-DoF aircraft model and implementing hardware-in-the-loop and flight-test validation on the ARCHER platform.

REFERENCES

[1] T. J. Koo and S. Sastry, Output Tracking Control Design of a Helicopter Model, *Proceedings of IEEE Conference on Decision Control,* pp. 3633-3638, 1999.
[2] R. Beard and T. McLain, *Small Unmanned Aircraft: Theory and Practice*, Princeton University Press, 2012.
[3] M. Napolitano, *Aircraft Dynamics: From Modeling to Simulation*, Wiley, 2014.
[4] S. Waslander, Unmanned Aircraft Systems: Control Challenges, *IEEE Control Sysy. Mag.,* vol. **37**, no. 3, pp. 46-74, 2017.
[5] E. Lavretsky and K. A. Wise, *Robust and Adaptive Control: Theory and Applications*, Springer, 2013.
[6] D. McFarlane and K. Glover, A loop-Shaping Design Procedure using H_inf Synthesis, *IEEE Trans. Autom. Control,* vol. **37**, no. 6, pp. 759-769, 1992.
[7] K. Zhou, J. Doyle and K. Glover, *Robust and Optimal Control*, Prentice Hall, 1996.
[8] M. Green and D. Limebeer, *Linear Robust Control*, Prentice Hall, 1995.
[9] D. O. Anderson and J. B. Moore, *Optimal Control: Linear Quadratic Methods*, Prentice Hall, 1990.
[10] A. Saberi, A. A. Stoorvogel and P. Sannuti, *Control of LinearSystems with Regulation and Input Constraints*, Springer, 2000.
[11] J. Shamma and M. Athans, Gain Scheduling: Potential Hazardsand possible Remedies, *IEEE Control Syst. Mag.,* vol. **12**, no. 3, pp. 101-107, 1992.
[12] J. Mohammadpour and C. Scherer, *Control of Linear Parameter Varying Systems with Applications*, Springer, 2012.
[13] P. Apkarian and R. J. Adams, Advanced Gain-Scheduling Tehniques for Uncertain Systems, *IEEE Trans. Control Syst. Technol.,* vol. **6**, no. 1, pp. 21-32, 1998.
[14] F. Wu, A Generalized LPV System Representation and its Application to Gain Scheduling, *Automatica,* vol. **38**, no. 9, pp. 1485-1494, 2002.
[15] A. M. Stoica, *Disturbance Attenuation and its Applications*, Editura Academiei, 2004.
[16] S. Skogestad and I. Postlethwaite, *Multivariable Feedback Control: Analysis and Design*, Wiley, 2005.